

MULTIGRID METHODS FOR PROBLEMS WITH A
SMALL PARAMETER IN THE HIGHEST DERIVATIVE

P.W. Hemker

1. INTRODUCTION

Much progress has been made recently in developing multigrid (MG-) methods to solve the systems of equations that arise from discretization of truly elliptic PDEs. Often the emphasis lies upon the search for the most efficient variant. However, for the MG-methods to be generally applied, it is important that the methods are not only efficient, but also that they do not fail or do not need particular adaptation for special cases of the general elliptic equation. Therefore, in this paper, we consider the elliptic equation when it degenerates because a coefficient in the highest derivative tends to zero and we study the behaviour of some MG-methods under these circumstances. Related problems are studied in [2,4,5,12,15,22].

Our main objective is the development of methods for the general linear 2nd order elliptic PDE with variable coefficients

$$\begin{aligned} Lu &\equiv -\nabla(\bar{\epsilon}\nabla u) + \bar{b}\nabla u + cu = f \quad \text{on } \Omega, \\ u &= g \quad \text{on } \Gamma_D, \quad \Omega \subset \mathbb{R}^2 \text{ bounded,} \\ \bar{n}\bar{\epsilon}\nabla u &= h \quad \text{on } \Gamma_N, \quad \Gamma_N \cup \Gamma_D = \delta\Omega. \end{aligned} \tag{1.1}$$

Here $\nabla = (\partial/\partial x, \partial/\partial y)$, and $\bar{\epsilon}$ is symmetric positive definite 2×2 matrix. The coefficients \bar{b} and c and the data f, g and h are real functions on Ω or $\partial\Omega$.

In particular our interest goes to cases where general methods easily fail: (i) $\bar{\epsilon}$ has *one* small eigenvalue and (ii) $\bar{\epsilon}$ has *two* small eigenvalues w.r.t. $|\bar{b}h|$, where h is a characteristic length (e.g. the meshsize). To investigate these cases in detail we consider two constant coefficient model problems. The first is the *anisotropic diffusion equation*:

$$L_\epsilon u \equiv -(\epsilon c^2 + s^2)u_{xx} - 2(\epsilon-1)scu_{xy} - (\epsilon s^2 + c^2)u_{yy} = f, \tag{1.2}$$

with $c = \cos(\alpha)$ and $s = \sin(\alpha)$. This equation is obtained from $-\bar{\epsilon}u_{xx} - u_{yy} = f$ by rotation with an angle α . The eigenvalues of $\bar{\epsilon}$ are 1 and ϵ . The second problem is the *convection-diffusion equation*:

$$L_\epsilon u \equiv -\epsilon(u_{xx} + u_{yy}) + cu_x + su_y = f. \tag{1.3}$$

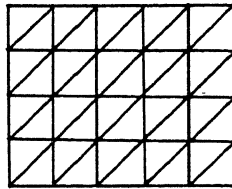
Here ϵ is a scalar coefficient and the convection direction is given by α .

We must keep in mind that in applications \bar{b} and c are variable coefficients and the direction of the anisotropy or the convection is a priori unknown. Therefore we

keep α as a parameter and we disregard the possibility of alignment of coordinate axes to the special direction in the equation.

Solutions of (1.2) and (1.3) may show layers, i.e. regions in which the solution varies rapidly. For (1.2) these layers may appear along lines in the direction of the strong diffusion. For (1.3) they may appear along the subcharacteristics or at the outflow boundary.

For the discretization of (1.1) we use methods of the finite element (FE) type. We assume that Ω can be covered by a triangularization T_h in a regular rectangular grid



and we use spaces of trialfunctions S^h and testfunctions V^h , such that the support of a basisfunction ϕ_i (or ψ_i) in S^h (or V^h) consists of only the triangles that are connected with the nodal point x_i .

For simple functions ϕ_i and ψ_i these discretizations

$$L_h u_h = f_h \tag{1.4}$$

yield coefficient matrices L_h with a regular 7-diagonal structure. The standard (FEM) method is with both ϕ_i and ψ_i continuous piecewise linear. The 7-point discretizations are the simplest ones by which also a cross-term derivative u_{xy} can be represented.

2. THE MULTIGRID ALGORITHM

The multigrid method considered here is an iterative process for the solution of (1.4). It makes use of a sequence of discretizations on grids coarser than used for $L_h u_h = f_h$. Each next coarser grid has a doubled meshsize and is obtained by leaving out each second meshline.

In the multigrid method (MGM) each iteration cycle consists of:

- 1.) p (pre-) relaxation sweeps;
- 2.) a coarse grid correction;
- 3.) q (post-) relaxation sweeps.

The coarse grid correction (GGC) consists of:

- a) the computation of the current residual, $r_h := f_h - L_h u_h$;
- b) the restriction of the residual to the next coarser grid, $r_H := \bar{R}_{Hh} r_h$;
- c) the computation of \tilde{c}_H , the approximate solution of the correction equation on a coarser grid:

$$L_H c_H = r_H, \quad (2.1)$$

by application of s MGM iteration cycles to this equation;

d) an update of the current solution u_h by addition of the prolonged (interpolated) correction

$$u_h := u_h + P_{hH} \tilde{c}_H.$$

By the recursive structure of this algorithm a coarsest grid exists on which the correction equation (2.1) has to be solved by another method (at choice). The coarse grid discrete operators L_H can be contained either by discretization, analogous to L_h , or by the construction of the *Galerkin approximation*

$$L_H = \bar{R}_{Hh} L_h P_{hH}. \quad (2.2)$$

We see that, beside the choice of the operator L_H , for a CGC we have to choose operators for the restriction (\bar{R}_{Hh}) and prolongation (P_{hH}). These operators are discussed in section 3.

If (2.1) is solved exactly, no coarser discretizations than L_H are involved, and the algorithm is a two-grid method (TGM). Its CGC is described by

$$u_h := u_h + P_{hH} L_H^{-1} \bar{R}_{Hh} (f_h - L_h u_h). \quad (2.3)$$

It can be shown [8] that under suitable conditions, for s large enough (roughly $s \geq 2$), the convergence behaviour of the MGM is almost the same as of the TGM. In practice, also $s = 1$ is often a good choice.

Most essential for the efficiency of the MGM is the choice of the relaxation method. Methods that are often used in this context are Point Gauss-Seidel relaxations (scanning the points in some order e.g. red-black or various lexicographical orderings), Line Gauss-Seidel relaxations (with different possible line-orderings, e.g. zebra or lexicographical [19]). Other relaxation methods are based on incomplete decompositions of the coefficient matrix, viz. Incomplete LU-decomposition (ILU-) relaxation or Incomplete Line-LU- (ILLU-) relaxation. All these relaxation methods are of the form

$$\tilde{L}_h u_h^{(i+1)} = \tilde{L}_h u_h^{(i)} - L_h u_h^{(i)} + f_h, \quad (2.4)$$

where \tilde{L}_h is an approximation to L_h .

For ILU relaxation, in each sweep a linear system is solved of the form

$$L U u_h^{(i+1)} = f_h + R u_h^{(i)},$$

where $\tilde{L}_h = LU = L_h - R$ is an approximate Crout-decomposition of L_h , with L and U lower and upper triangular matrices with the same sparsity structure as L_h [17,20].

For ILLU relaxation [15,16] in each sweep $u_h^{(i+1)}$ is solved from a system

$$(L + \bar{D}) \bar{D}^{-1} (\bar{D} + U) (u_h^{(i+1)} - u_h^{(i)}) = f_h - L_h u_h^{(i)}. \quad (2.5)$$

The matrices L , \bar{D} and U are obtained from the coefficient matrix L_h , written in block-tridiagonal form as

$$L_h = L + D + U = \begin{array}{|c|c|c|c|c|} \hline D_1 & U_1 & & & \\ \hline L_2 & D_2 & U_2 & & \\ \hline & L_3 & D_3 & \ddots & \\ \hline & & \ddots & \ddots & U_{n-1} \\ \hline & & & L_n & D_n \\ \hline \end{array}.$$

The block-diagonal matrix \bar{D} , with the same sparsity pattern as D , is computed recursively from

$$\begin{cases} \bar{D}_1 = D_1, \\ \bar{D}_j = D_j - \text{tridiag} (L_j \bar{D}_{j-1}^{-1} U_{j-1}), \quad j = 2, 3, \dots, n, \end{cases} \quad (2.6)$$

where tridiag is the operator which selects the tridiagonal submatrix from a dense matrix.

3. NESTED DISCRETIZATIONS

The relation between the discretizations on the different grids in a MGM can be considered analogous to the relation between the continuous and a discrete problem. For discretization of an equation $Lu = f$, ($L: X \rightarrow Y$, X and Y Banach spaces), we relate to it the discrete equation $L_h u_h = f_h$, ($L_h: X_h \rightarrow Y_h$). The relation between the two equations is made by the prolongation $P_h: X_h \rightarrow X$ (a linear injection) and the restrictions $R_h: X \rightarrow X_h$ and $\bar{R}_h: Y \rightarrow Y_h$ (linear surjections).

In the same way coarser discretizations $L_H u_H = f_H$ are related to finer $L_h u_h = f_h$ by a prolongation $P_{hH}: X_h \rightarrow X_H$ (linear injection), and restrictions $R_{hH}: X_H \rightarrow X_h$ and $\bar{R}_{hH}: Y_h \rightarrow Y_H$ (linear surjections). The coarse grid Galerkin approximation (2.2) is the analogue of the Galerkin discretization $L_h = \bar{R}_h L P_h$. A sequence of nested discretizations of a continuous equation $Lu = f$ is obtained by selecting prolongations and restrictions such that

$$P_H = P_h P_{hH}, \quad R_H = R_{hH} R_h, \quad \bar{R}_H = \bar{R}_{hH} \bar{R}_h. \quad (3.1)$$

In the standard FE discretization (sect. 1) the prolongation $P_h: X_h \rightarrow X$ is defined by linear interpolation over the triangles of T_h ; $R_h: X \rightarrow X_h$ is defined by injection (i.e. restriction of the function values to nodal points) and \bar{R}_h is defined by weighting by the continuous piecewise linear basis-functions $\phi_i^h \in V^h$:

$$(\bar{R}_h f)_i \equiv (f_h)_i \equiv \int f(x) \phi_i^h(x) d\Omega. \quad (3.2)$$

The FE discretization corresponds to the Galerkin discretization $L_h = \bar{R}_h L P_h$.

To obtain a sequence of nested discretizations related with the FE discretization, we use a corresponding P_{hH} and \bar{R}_{hH} . The prolongation P_{hH} should satisfy (3.1) with linear interpolation for P_h and P_H . Hence,

$$P_{hH} u_H = \sum_j u_j^H \phi_j^H = \sum_{j,i} u_j^H r_{ji}^H \phi_i^h = \sum_i \left(\sum_j r_{ji}^H u_j^H \right) \phi_i^h = P_{hH}^* P_{hH} u_h.$$

Therefore, P_{hH} is given by the prolongation molecule

$$P_{hH}^* = (r_{ji}) = \begin{bmatrix} & \frac{1}{2} & \frac{1}{2} \\ \frac{1}{2} & 1 & \\ \frac{1}{2} & & \frac{1}{2} \end{bmatrix}. \tag{3.3}$$

For \bar{R}_{Hh} we have

$$(\bar{R}_{Hh} f_h)_i = (f_H)_i = \int f(x) \phi_i^H(x) d\Omega = \int f \sum_j r_{ij}^H \phi_j^h d\Omega = \sum_j r_{ij}^H (f_h)_j;$$

the restriction molecule \bar{R}_{Hh}^* of \bar{R}_{Hh} is also given by (3.3). In this case $\bar{R}_{Hh} = (P_{hH})^T$. These P_{hH} and \bar{R}_{Hh} are the same 7-point prolongation and restriction as introduced in [20,21]. For points near the boundary obvious modifications of the molecules have to be made.

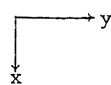
With the P_{hH} and \bar{R}_{Hh} given by (3.3), the FE discretization on the different levels form a nested sequence and L_H can be computed from L_h by (2.2):

$$L_H = \bar{R}_H L_h P_H = \bar{R}_{Hh} \bar{R}_h L_h P_h P_H = \bar{R}_{Hh} L_h P_{hH}. \tag{3.4}$$

Starting with the discretization L_h on N meshpoints, and using (3.3) for \bar{R}_{Hh} and P_{hH} , it takes less than $29 N$ additions and $7/3 N$ multiplications to compute the discrete operators on *all* coarser grids.

Application of FEM to the constant coefficient equation (1.1) on an equidistant regular T_h yields the 7-point difference molecules

$$-h^2 \left(\frac{\partial}{\partial x} \right)^2 \sim \begin{bmatrix} -1 & 0 \\ 0 & 2 & 0 \\ 0 & -1 \end{bmatrix} = A_{11}^*, \quad -h^2 \left(\frac{\partial}{\partial y} \right)^2 \sim \begin{bmatrix} 0 & 0 \\ -1 & 2 & -1 \\ 0 & 0 \end{bmatrix} = A_{22}^*, \tag{3.5}$$

$$-2h^2 \left(\frac{\partial}{\partial x} \right) \left(\frac{\partial}{\partial y} \right) \sim \begin{bmatrix} 1 & -1 \\ 1 & -2 & 1 \\ -1 & 1 \end{bmatrix} = A_{12}^*,$$


the 2nd order terms; and

$$6h \left(\frac{\partial}{\partial x} \right) \sim \begin{bmatrix} -2 & -1 \\ -1 & 0 & 1 \\ 1 & 2 \end{bmatrix} = A_1^*, \quad 6h \left(\frac{\partial}{\partial y} \right) \sim \begin{bmatrix} -1 & 1 \\ -2 & 0 & 2 \\ -1 & 1 \end{bmatrix} = A_2^*, \tag{3.6}$$

the 1st order terms; and

$$12I \sim \begin{bmatrix} 1 & 1 \\ 1 & 6 & 1 \\ 1 & 1 \end{bmatrix} = A_0^*. \tag{3.7}$$

the 0th order term.

For each p -th order difference molecule A_h^* in (3.5)-(3.7) we find ($H=2h$)

$$\bar{R}_{Hh}^* A_h^* P_{hH}^* = 2^{2-p} A_{2h}^*, \tag{3.8}$$

where $***$ denotes the combined application of the prolongation and restriction (i.e.

convolution and contraction of the molecules). This means that the difference molecules (3.5)-(3.7) are all invariant under Galerkin approximation. The factor 2^{2-p} takes into account the difference in meshsize on the different levels. A 7th linearly independent 7-point molecule,

$$A_3^* = \begin{bmatrix} -1 & 1 \\ 1 & 0 & -1 \\ -1 & 1 \end{bmatrix} \sim h^3 \left(\frac{\partial}{\partial t} \right) \left(\frac{\partial}{\partial y} \right) \left(\frac{\partial}{\partial x} - \frac{\partial}{\partial y} \right), \quad (3.9)$$

satisfies (3.8) with $p = 3$.

It follows that other than FEM molecules are *not* invariant under Galerkin approximation with \bar{R}_{Hh} and P_{Hh} given by (3.3). Examples are:

1) the central difference operator

$$6h \left(\frac{\partial}{\partial x} \right) \sim A_1^* + A_3^*; \quad (3.10)$$

2) the upwind difference operator

$$6h \left(\frac{\partial}{\partial x} \right) \sim U_1^* = A_1^* + A_3^* + 3A_{11}^*. \quad (3.11)$$

For any of these discretizations on the finest grid, the repeated use of (2.2) with the P_{Hh} and \bar{R}_{Hh} given by (3.3), yields discretizations on coarser grids that tend to the FE discretization. E.g., for (3.11) k times application of (3.8) yields

$$(R^* *)^k (hU_1^*)^k (*P^*)^k = 2^k h [A_1^* + 2^{-2k} A_3^* + 3 \cdot 2^{-k} A_{11}^*], \quad (3.12)$$

which tends to $2^k h A_1^*$ as k increases.

4. THE ANISOTROPIC DIFFUSION EQUATION

The 7-point molecule for (1.2) obtained by FEM reads

$$L_{h,\varepsilon}^* = \begin{bmatrix} & s(c-s) & -sc \\ c(s-c) & 2-2sc & c(s-c) \\ -sc & s(c-s) & \end{bmatrix} + \varepsilon \begin{bmatrix} & -c(s+c) & sc \\ -s(s+c) & 2+2sc & -s(s+c) \\ sc & -c(s+c) & \end{bmatrix}. \quad (4.1)$$

To investigate the relaxation methods for (4.1) we use Local Mode Analysis [19], i.e. we consider the discretization on an infinite domain (or on a finite domain with periodic boundary conditions). For the linear constant coefficient (difference) operator L (or L_h) its symbol $\hat{L}(\omega)$ (or $\hat{L}_h(\omega)$) is introduced by

$$Lu_\omega = \hat{L}(\omega)u_\omega \quad \text{or} \quad L_h u_\omega = \hat{L}_h(\omega)u_\omega,$$

where

$$u_\omega(x,y) = e^{i(\omega_1 x + \omega_2 y)},$$

$$\hat{L}: \mathbb{R}^2 \rightarrow \mathbb{C},$$

$$\hat{L}_h: T_h^2 \equiv [-\pi/h, \pi/h]^2 \rightarrow \mathbb{C}.$$

T_h^2 is the domain of all frequencies ω that are visible on a grid with meshsize h . For convenience we use also the notation $\phi = h\omega_1$, $\theta = h\omega_2$, and $u_\omega = u_{\phi,\theta}$.

For equation (1.2) we find the symbol

$$h^2 \widehat{L}_\varepsilon(\phi, \theta) = (s\phi - c\theta)^2 + \varepsilon(c\phi + s\theta)^2. \quad (4.2)$$

For $\varepsilon > 0$, $(\phi, \theta) \neq (0, 0)$ we have $\widehat{L}_\varepsilon(\omega) > 0$, which shows the ellipticity of L_ε . For the reduced case, $\varepsilon = 0$, we have

$$L_\varepsilon(\phi, \theta) = 0 \text{ iff } s\phi = c\theta. \quad (4.3)$$

This problem is not longer elliptic and it has *unstable modes* $u_{\phi, \theta}$ for (ϕ, θ) satisfying (4.3). For the discretized problem (1.2), we derive from (4.1)

$$\begin{aligned} \widehat{L}_{h, \varepsilon}(\phi, \theta) = & [s + (c-s)\cos\phi - c\cos(\phi-\theta)]^2 + [(c-s)\sin\phi - c\sin(\phi-\theta)]^2 \\ & + \varepsilon[-(c+s)\cos\phi + s\cos(\phi-\theta)]^2 + \varepsilon[(c+s)\sin\phi - s\sin(\phi-\theta)]^2. \end{aligned} \quad (4.4)$$

Again $\widehat{L}_{h, \varepsilon}(\phi, \theta) > 0$ for $\varepsilon > 0$, $(\phi, \theta) \neq (0, 0)$, but for $\varepsilon = 0$ we see

$$\begin{aligned} \widehat{L}_{h, 0}(\phi, \theta) = 0 \text{ iff} \quad & \text{(i) } \phi = \theta = 0, \\ & \text{or (ii) } \phi = 0 \text{ and } c = 0, \\ & \text{or (iii) } \theta = 0 \text{ and } s = 0, \\ & \text{or (iv) } \phi = \theta \text{ and } s = c. \end{aligned} \quad (4.5)$$

Except for $\phi = \theta = 0$, the discrete operator has unstable modes *only* if the direction of the strong diffusion is along one of the (three) gridline directions. For all other α we find $L_{L, 0}(\phi, \theta) > 0$ for $(\phi, \theta) \neq (0, 0)$. If the strong diffusion is *not* along the gridlines, the discrete scheme is elliptic where the original operator is not. The discretization introduces artificial cross-diffusion.

For $\alpha \neq 0, \pi/4, \pi/2$, this extra stability guarantees the existence of a relaxation method for its solution [6] (viz. a properly damped Jacobi relaxation). How to find an efficient relaxation, however, is not immediately clear. This is particularly so because (4.1) does not yield an L-matrix (non-negative off-diagonal elements) for all ε and α , and hence e.g. ILU-relaxation may diverge. The domain in the α - ε -plane where $L_{h, \varepsilon}$ is an L-matrix is shown in figure 4.1.

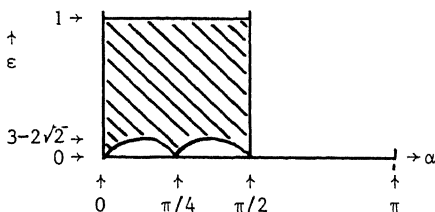


Fig. 4.1. The shaded area denotes the domain in the (α, ε) -plane where (4.1) yields an L-matrix.

We see that $\alpha = 0, \pi/4, \pi/2$ play again a special role. Therefore in numerical experiments more angles α have to be considered to obtain an insight in the general behaviour of the smoothing processes. Here, to examine the relaxation methods, we compute the smoothing factor (cf. [19] sect. 7) for various (α, ε) , for lexicographical Gauss-Seidel, zebra, ILU and ILLU relaxation. The smoothing factor gives a first

impression of the rate of convergence of a MGM with $p + q = 1$.

$\alpha \backslash \epsilon$	PGS		zebra		ILU		ILLU	
	1.0(-2)	1.0(-4)	1.0(-2)	1.0(-4)	1.0(-2)	1.0(-4)	1.0(-2)	1.0(-4)
0°	<u>0.980</u>	<u>1.000</u>	<u>0.125</u>	<u>0.125</u>	<u>0.607</u>	<u>0.946</u>	<u>0.1759</u>	<u>1.97(-1)</u>
$7\frac{1}{2}^\circ$	0.963	0.984	0.472	0.660	2.469!	6.855!	0.0607	2.97(-5)
15°	0.928	0.948	0.659	0.727	1.352!	1.735!	0.0152	3.05(-6)
22.5	0.902	0.924	0.751	0.803	0.711	0.767	0.0069	1.19(-6)
30	0.885	0.910	0.838	0.884	0.701	0.767	0.0127	2.81(-6)
37.5	0.908	0.957	0.911	0.960	1.138!	2.283!	0.0418	2.04(-5)
45	<u>0.925</u>	<u>0.999</u>	<u>0.943</u>	<u>0.999</u>	<u>0.497</u>	<u>0.92</u>	<u>0.1323</u>	<u>1.64(-1)</u>
52.5	0.897	0.949	0.887	0.943	0.044	1.68(-5)	0.0536	4.08(-5)
60	0.871	0.908	0.838	0.874	0.0192	4.02(-6)	0.0196	5.35(-6)
67.5	0.882	0.910	0.867	0.894	0.0168	3.29(-6)	0.0165	3.94(-6)
75	0.921	0.944	0.915	0.940	0.0264	6.56(-6)	0.0239	6.94(-6)
82.5	0.962	0.983	0.961	0.983	0.0728	5.26(-5)	0.0641	5.25(-5)
90	<u>0.980</u>	<u>1.000</u>	<u>0.980</u>	<u>1.000</u>	<u>0.1709</u>	<u>0.1716</u>	<u>0.1490</u>	<u>0.1692</u>
97.5	0.967	0.983	0.966	0.982	0.0420	2.36(-5)	0.0350	1.96(-5)
105	0.927	0.940	0.921	0.935	6.92(-3)	1.27(-6)	5.17(-3)	4.69(-7)
112.5	0.874	0.884	0.845	0.857	1.71(-3)	2.28(-7)	1.16(-3)	1.06(-7)
120	0.819	0.826	0.763	0.773	6.56(-4)	7.78(-8)	3.82(-4)	1.19(-7)
127.5	0.769	0.774	0.661	0.668	3.33(-4)	3.76(-8)	1.69(-4)	6.50(-8)
135	0.724	0.727	0.547	0.553	2.20(-4)	2.41(-8)	1.87(-4)	6.53(-8)
142.5	0.685	0.691	0.427	0.431	3.13(-4)	3.47(-8)	2.76(-4)	1.19(-7)
150	0.777	0.786	0.397	0.411	5.63(-4)	6.44(-8)	5.26(-4)	1.15(-7)
157.5	0.859	0.870	0.432	0.454	1.32(-3)	1.63(-7)	1.38(-3)	2.11(-7)
165	0.923	0.937	0.451	0.501	4.42(-3)	6.50(-7)	5.62(-3)	9.50(-7)
172.5	0.966	0.983	0.394	0.543	0.0275	7.99(-6)	0.0396	1.62(-5)

Table 4.1 Smoothing factors by Local Mode Analysis of lexicographic Point Gauss-Seidel, zebra, ILU and ILLU relaxation for (4.1).

From table 4.1 we see that Gauss-Seidel relaxation is slow for small ϵ , zebra smoothing is essentially better. For angles $\pi/4 \leq \alpha \leq \pi$ the ILU is an excellent smoother, but for $0 < \alpha < \pi/4$ it is unreliable and may diverge. This divergence, found by local mode analysis, appears for modes $u_{\phi, \theta}$ with $(\phi, \theta) \approx (0, \pi)$ if $0 < \alpha < \pi/8$ and for $(\phi, \theta) \approx (-\pi, \pi)$ if $\pi/8 < \alpha < \pi/4$. The same modes are also found to diverge in real MGM-iterations if a fine enough grid is used. The ILLU relaxation converges rapidly in all cases.

That ILU is a good smoother for $\pi/4 < \alpha < \pi$ for all ϵ can be explained by the fact that (4.1) with $\epsilon = 0$ can be decomposed into a product of two molecules corresponding to the LU decomposition. Two of these decompositions are possible

$$\begin{bmatrix} & s(c-s) & -cs \\ c(s-c) & 2-2cs & c(s-c) \\ -cs & s(c-s) & \end{bmatrix} = \begin{bmatrix} & s(c-s) & 0 \\ c(s-c) & (s-c)^2 & 0 \\ 0 & 0 & \end{bmatrix} * \begin{bmatrix} 0 & 0 \\ 0 & 1 \\ 0 & \frac{-s}{s-c} & \frac{c}{s-c} \end{bmatrix} \quad (4.6)$$

$$= \begin{bmatrix} & s(c-s) & -cs \\ 0 & s^2 & 0 \\ 0 & 0 & \end{bmatrix} * \begin{bmatrix} 0 & 0 \\ 0 & 1 \\ -c/s & \frac{c-s}{s} & 0 \end{bmatrix} \quad (4.7)$$

Decomposition (4.7) has a bounded inverse for $\pi/4 < \alpha < \pi/2$ and (4.6) for $\pi/2 < \alpha < \pi$. For these ranges of α , the corresponding decompositions are also those found by the LU-decomposition algorithm as described in [20,21]. However, neither (4.6) nor (4.7) is found for $0 < \alpha < \pi/4$. For small ϵ the decompositions (4.6) and (4.7) are found asymptotically. For $\epsilon \rightarrow 0$ they approximate L and U up to $O(\epsilon)$. Therefore, for $\pi/4 < \alpha < \pi$, the ILU-decomposition LU is an accurate approximation to $L_{h,\epsilon}$ for small ϵ . Hence ILU is a good smoother (only) in these cases.

To explain the small smoothing factor for the ILLU relaxation we consider (2.5) -(2.6) and we introduce the molecules

$$\begin{aligned} L^* &= [0, \quad s(c-s), \quad -sc \quad], \\ D^* &= [c(s-c), \quad 2-2cs, \quad c(s-c)], \\ U^* &= [-sc, \quad s(c-s), \quad 0 \quad]. \end{aligned}$$

We compute \bar{D}^* from $\bar{D}^*(\bar{D}^*-D^*) + L^*U^* = 0$ and obtain

$$\bar{D}^* = [c(s-c), \quad (c-s)^2 + c^2, \quad c(s-c)].$$

This \bar{D}^* corresponds to a tridiagonal matrix and has a bounded inverse for all α . Therefore, it is also a solution of

$$\bar{D}^* = D^* - \text{tridiag} (L^*(\bar{D}^*)^{-1}U^*),$$

and we find that this ILU-decomposition is exact for $\epsilon = 0$:

$$\tilde{L}_{h,0}^* = (L^* + \bar{D}^*)(\bar{D}^*)^{-1}(\bar{D}^* + U^*) = L^* + D^* + U^* = L_{h,0}^*.$$

For small ϵ the ILLU-decomposition algorithm generates this decomposition asymptotically (away from the boundary). This explains why ILLU is an excellent smoother for small ϵ and all α .

5. THE CONVECTION DIFFUSION EQUATION

The direct application of the standard FEM to equation (1.3) yields inadequate discretizations for small ϵ/h [3,13,18]. The same is true for central differences. Therefore, either direction-dependent (upwind-) differences are used or an artificial diffusion is introduced. For the solution of the discrete systems the MG-method can

be applied. However, due to the special character of the equations, typical difficulties may arise. These have been studied for upwind differences in [5,12,16] and for artificial diffusion in [4,5,22].

In this section we make some remarks on the application of artificial diffusion. In section 6 we consider a MG-variant consistent with the Streamline-Upwind FE-method [7,14].

Molecules for the discretization of (1.3) are given by

$$L_{\gamma,h}^* = \gamma(A_{11}^* + A_{22}^*) + \frac{hc}{6}(A_1^* + pA_3^*) + \frac{hs}{6}(A_2^* - pA_3^*). \quad (5.1)$$

For finite elements $p = 0$, for central differences $p = 1$; $\gamma = \gamma(h) = \varepsilon + \beta h$ is the diffusion coefficient, β or $\beta(h)$ is the coefficient of artificial diffusion.

The symbol of $L_{\gamma,h}$ is given by

$$\hat{L}_{\gamma,h}(\phi, \theta) = 4\gamma[\sin^2(\phi/2) + \sin^2(\theta/2)] + ihT(\phi, \theta), \quad (5.2)$$

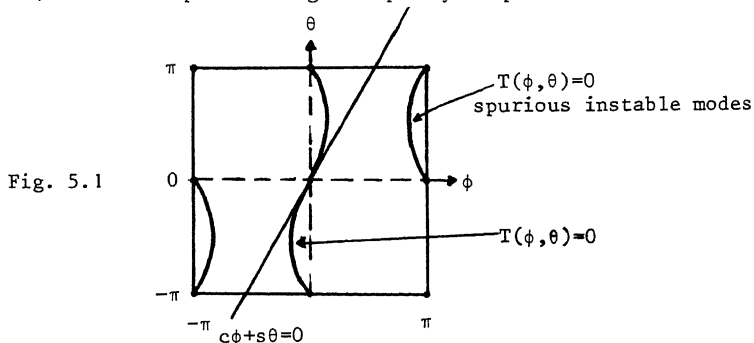
with

$$T(\phi, \theta) = c \sin(\phi/2)[2 \cos(\phi/2) + (1-p)\cos(\theta-\phi/2)] + s \sin(\theta/2)[2 \cos(\theta/2) + (1-p)\cos(\phi-\theta/2)]. \quad (5.3)$$

For the continuous operator (1.3) we have

$$\hat{L}_\varepsilon(\phi, \theta) = \varepsilon(\phi^2 + \theta^2) + ih(c\phi + s\theta).$$

Hence, for (1.3) with $\varepsilon = 0$, unstable modes $u_{\phi, \theta}$ exist for (ϕ, θ) with $c\phi + s\theta = 0$. I.e. the reduced continuous operator has one set of unstable modes. (In the solution these components are determined by the inflow boundary data.) For (5.2) with $\gamma = 0$ we find two branches of unstable modes. A branch of spurious unstable modes is found in the high frequency domain (figure 5.1). This implies that relaxation methods of the form (2.4) do not damp these high frequency components.



From (5.2) it follows that the discretization (5.1) is stable if $\gamma \geq Ch > 0$ (cf. [22]). For such stable discretizations the existence of a relaxation method which damps the high frequencies in the error is guaranteed (cf. [6]). It is of practical

importance to find relaxations that work efficiently. To compare the effect of some relaxations, in table 5.1 we give smoothing factors for zebra, ILU and ILLU relaxation, when applied to (5.1) with $p = 0$; $\gamma(h) = \epsilon + \beta h$; $\epsilon = 0$; $\beta = 0.5, 1$.

α	zebra		ILU		ILLU	
	$\beta = 0.5$	$\beta = 1.0$	$\beta = 0.5$	$\beta = 1.0$	$\beta = 0.5$	$\beta = 1.0$
0°	0.711	0.280	0.0777	0.0937	0.0221	0.0257
30°	0.584	0.245	0.0148	0.0837	0.0021	0.0366
60°	0.286	0.243	0.0754	0.100	0.0601	0.0611
90°	0.252	0.250	0.195	0.127	0.1063	0.0746
120°	0.290	0.260	0.237	0.139	0.0674	0.0607
150°	0.573	0.263	0.160	0.123	0.0324	0.0364

Table 5.1 Smoothing rates for FE discretization of (1.3) with $\epsilon = 0$ and with artificial diffusion $\gamma = \beta h$.

In the MGM not only the smoothing should efficiently damp the high frequencies in the error, but also the CGC should work properly to reduce the low frequencies. For equation (1.3) this CGC needs special attention. From section 3 we know that application of (2.2) to $L_{\gamma(h),h}$, with P_{hH} and \bar{R}_{Hh} given by (3.3), yields on a coarser level

$$\bar{R}_{2h,h}^L L_{\gamma(h),h}^P P_{h,2h} = L_{\gamma(h),2h},$$

i.e. the FE discrete operator on the grid $2h$ with diffusion coefficient $\gamma(h)$. This means that the Galerkin approximation gives an amount of diffusion on the coarse grids that is equal to the amount used at the finer grids. When repeatedly applied, this produces a FE discretization with negligible artificial diffusion on the coarsest grids. Hence, the coarser grid operators become unstable, and diverging corrections will appear in the CGCs.

To avoid the unstable Galerkin approximations, we can discretize the problem on each grid - with meshsize H - with a corresponding artificial diffusion $\gamma(H)$. This is studied in [22], where suggestions are given for the choice of $\gamma(h)$ on the different levels. However, the lack of consistency between the diffusion terms in the discrete operators affects the convergence rate of the CGC. By the same argument as used in [5, p40], it is found that the reduction of some low-frequency components is only by a factor $(\gamma(H) - \gamma(h)) / \gamma(H)$ when in a CGC the operators $L_{\gamma(h),h}$ and $L_{\gamma(H),H}$ are used.

6. A STREAMLINE-UPWIND RESTRICTION FOR THE CONVECTION DIFFUSION EQUATION

In this section we introduce a new, asymmetric restriction. This restriction is

applied in combination with the Streamline-Upwind Petrov-Galerkin (SU-PG) FE method of discretization [7,14] and, in fact, it is the discrete analogue of the asymmetric weight-function in that method. With this \bar{R}_{Hh} in (2.2) we obtain Galerkin coarse grid operators that are again of the Streamline-Upwind type. Other asymmetric restrictions have been studied for finite difference methods in [1,12,16]. These restrictions satisfy $\bar{R}_{Hh} = P_{hH}^T$ where the interpolation P_{hH} is deduced from the difference equation (matrix-weighted interpolation). The comparison of the different asymmetric methods might be the subject of future study. Here, with the new restriction, we remain consistent with the Petrov-Galerkin approach [7,14]: the prolongation is kept unchanged and only the restriction is adapted to the differential equation.

The SU-PG method is a FE method for the solution of (1.1) with trialfunctions $S^h = \text{span}\{\phi_j^h\}$ and testfunctions $V^h = \text{span}\{\phi_j^h + k\bar{b}\nabla\phi_j^h\}$. The functions ϕ_j^h are standard FE basis-functions. We apply the method with piecewise linear ϕ_j^h on the triangularization T^h ; $k = k(h, \epsilon)$ is a scalar parameter. It can be shown [11] that a good choice of $k(h, \epsilon)$ should satisfy

$$k(h) = O(h) \quad \text{if } \epsilon/h \leq C, \quad k(h) = O(h^2/\epsilon) \quad \text{if } \epsilon/h \geq C.$$

For (1.3) we obtain the discrete equations

$$\sum_j B(\phi_i, \phi_j) u_j^h = \ell(\phi_i), \quad (6.1)$$

where

$$B(\phi_i, \phi_j) = \sum_e \int \nabla \phi_i (\epsilon I + k\bar{b}^{-T}\bar{b}) \nabla \phi_j + \phi_i \bar{b} \nabla \phi_j d\Omega_e, \quad (6.2)$$

$$\ell(\phi_i) = \sum_e \int (\phi_i + k\bar{b} \nabla \phi_i) f d\Omega_e. \quad (6.3)$$

The differences with standard FEM are:

1) an anisotropic (streamline directed) artificial diffusion appears:

$$\bar{\gamma}(h) = \epsilon I + k(h)\bar{b}^{-T}\bar{b}; \quad (6.4)$$

2) the functions in the space Y are weighted by an asymmetric (upwind weighted) weight function.

The weighting of the space Y defines an asymmetric restriction \bar{R}_h and for a piecewise polynomial approximation of functions in Y , restriction molecules can be derived.

For instance, if Y is approximated by piecewise linear functions on T_h , this restriction molecule reads

$$\bar{R}_h^* = \frac{h^2}{6} \{ \frac{1}{2} A_0^* + k b_1 A_1^* + k b_2 A_2^* \}. \quad (6.5)$$

This asymmetric molecule suggests an asymmetric restriction \bar{R}_{Hh} with a molecule

$$\bar{R}_{Hh}^* = P_{hH}^* + \mu_1 (A_1^* + pA_3^*) + \mu_2 (A_2^* - pA_3^*) \quad (6.6)$$

(e.g. $p = 0$ or $p = 1$). The difference molecule corresponding with the discrete operator (6.2) reads

$$h^2 L_h^* = \gamma_{11} A_{11}^* + \gamma_{12} A_{12}^* + \gamma_{22} A_{22}^* + \frac{hb_1}{6} A_1^* + \frac{hb_2}{6} A_2^*. \quad (6.7)$$

When (6.6), (6.7) and (3.3) are used for the construction of a Galerkin approximation (2.2) we find the molecule

$$\begin{aligned} (2h)^2 \bar{R}_{hh}^* * L_h^* * P_{hH}^* &= (\gamma_{11} - \frac{3h\mu_1 b_1}{2}) A_{11}^* + (\gamma_{12} - \frac{3h}{2} \frac{\mu_1 b_2 + \mu_2 b_1}{2}) A_{12}^* + \\ &+ (\gamma_{22} - \frac{3h}{2} \mu_2 b_2) A_{22}^* + \frac{h}{3} (b_1 A_1^* + b_2 A_2^*) + r(\vec{b}, p) A_3^*. \end{aligned} \quad (6.8)$$

This is a discretization on the mesh $H = 2h$ of the same form as (6.7) except for the remainder term $r(\vec{b}, p) A_3^*$. We see that (6.8) has the additional amount of artificial diffusion

$$\gamma(2h) - \gamma(h) = -\frac{3h}{2} \begin{pmatrix} b_1 \\ b_2 \end{pmatrix} (\mu_1, \mu_2).$$

This is accounted for by the h -dependence of the parameter k . For (6.7) and (6.8) to be consistent with (6.4) the following relation is to be satisfied

$$[k(2h) - k(h)] \bar{b}^T \bar{b} = -\frac{3h}{2} \begin{pmatrix} b_1 \\ b_2 \end{pmatrix} (\mu_1, \mu_2).$$

Introducing the notation $\mu_j = -\frac{2}{3} \mu(h) b_j$, $j = 1, 2$, this relation reads

$$k(2h) - k(h) = h\mu(h). \quad (6.9)$$

Thus, our restriction (6.6) is upwind weighted and equation (6.9) shows how the parameters μ_k in the asymmetric restriction are related to the choice of the artificial streamline-diffusion parameter $k(h)$.

With this asymmetric \bar{R}_{hh} we expect the MGM to improve for the SU-PG discretization of (1.3) because (i) the CGCs use streamline-upwind Galerkin approximations as coarse grid operators and (ii) by the asymmetric restriction downstream residuals have less upstream influence.

An experiment was made to see the effects. The problem (1.3) was solved for $\epsilon = 10^{-3}$, on the unit square, using a MGM cycle with $(p, q, s) = (1, 0, 2)$ and with 5 levels of discretization ($h=1/32$ on the finest mesh; $k(h) = 2h/3$). Both the solution and the initial error were smooth. To see the effect of the new CGC a relaxation was used (zebra) with little capacity to reduce the low frequency error in the direction $\alpha = 0^\circ$ or 180° . Another experiment was made with the ILLU-relaxation (table 6.1).

L_H	zebra				ILLU			
	(2.2)	(2.2)	(6.2)	(6.2)	(2.2)	(2.2)	(6.2)	(6.2)
\bar{R}_{Hh}	(3.3)	(6.6)	(3.3)	(6.6)	(3.3)	(6.6)	(3.3)	(6.6)
α		p=0		p=0		p=0		p=0
0°	<u>div</u>	2.1	2.1	2.1	88.4	72.8	78.5	75.2
22.5°	2.0	1.8	1.9	1.8	29.9	14.6	24.5	14.7
45	2.1	2.6	2.5	2.6	23.7	10.7	16.1	10.7
67.5	2.4	5.4	2.9	4.3	19.0	13.8	16.8	14.8
90	4.9	5.0	4.5	4.9	29.7	25.8	26.7	25.9
112.5	2.0	2.9	2.1	2.9	27.9	25.3	23.7	25.0
135	<u>div</u>	3.9	1.5	4.0	124.	111.	112.	111.
157.5	<u>div</u>	2.9	1.7	2.9	116.	104.	104.	104.
180	<u>div</u>	2.4	1.7	2.3	41.4	36.2	35.8	36.4
202.5	1.7	2.4	1.9	2.3	19.3	11.8	14.1	14.4
225	1.7	2.9	1.7	2.9	21.7	14.3	15.0	14.3
247.5	2.1	3.5	2.5	3.2	21.2	17.6	15.8	16.4
270	4.4	4.2	3.8	4.2	29.1	25.6	25.7	25.5
292.5	<u>div</u>	2.2	1.4	2.2	17.1	13.9	15.4	14.1
315	<u>div</u>	3.6	1.8	3.6	87.6	74.7	78.0	74.7
337.5	<u>div</u>	3.4	2.3	3.3	150.	124.	125.	126.

Table 6.1 Residual convergence factors

$$\sqrt[3]{\|f_h - L_h u_h^{(2)}\|_2 / \|f_h - L_h u_h^{(5)}\|_2}.$$

Table 6.1 shows that the Galerkin approximation (2.2) with the symmetric \bar{R}_{Hh} , eq. (3.3), may diverge indeed. When the asymmetric \bar{R}_{Hh} , eq. (6.6), is used, little difference is seen between the CGCs with discretizations (2.2) or (6.2), as was expected from (6.8). In the case of zebra-relaxation the use of the asymmetric restriction has a positive effect. (Similar results were obtained for problems with boundary layers.) If we use the more powerful ILLU-relaxation, we see that the new CGC becomes of little importance. It even has an adverse effect. Now Galerkin approximation with the symmetric \bar{R}_{Hh} shows the best convergence rate. (This effect may disappear if more levels of discretization are used, cf. [22].) Apparently the ILLU-relaxation reduces the total error very efficiently. It also takes care of the low frequency components that are produced by the less stable (and more accurate) CGC obtained by the symmetric Galerkin approximation. This effect is seen for all flow directions α .

REFERENCES

- [1] ALCOUFFE, R.E., A. BRANDT, J.E. DENDY Jr. & J.W. PAINTER, *The multigrid method for the diffusion equation with strongly discontinuous coefficients*, SIAM J.S.S.C. 2 (1981) 430-454.
- [2] ASSELT, E.J. van, *The multigrid method and artificial viscosity*, In [9], pp. 313-326.
- [3] AXELSSON, O., L.S. FRANK & A. van der SLUIS, *Analytical and Numerical Approaches to Asymptotic Problems in Analysis*, North-Holland Publ. Comp., Amsterdam-New York, 1981.
- [4] BÖRGERS, C., *Mehrgitterverfahren für eine Mehrstellendiskretisierung der Poissongleichung und für eine zweidimensionale singulär gestörte Aufgabe*, Diplomarbeit, Institut für Angewandte Mathematik, Universität Bonn, 1981.
- [5] BRANDT, A., *Multigrid solvers for non-elliptic and singular perturbation steady-state problems*, Research Report, Dept. of Applied Mathematics, Weizmann Institute of Science, Rehovot, Israel, 1981.
- [6] BRANDT, A., *Numerical stability and fast solutions to boundary value problems*, In [18], pp. 29-49.
- [7] BROOKS, A.N. & T.J.R. HUGHES, *Streamline-Upwind Petrov-Galerkin Formulations for Convection Dominated Flows with Particular Emphasis on the Incompressible Navier-Stokes Equations*, Comp. Meth. Appl. Mech. Engng. 32 (1982) pp. 199-259.
- [8] HACKBUSCH, W., *On the convergence of a multigrid iteration applied to finite element equations*, Report 77-8, Inst. Angew. Math., Univ. Köln, 1977.
- [9] HACKBUSCH, W. & U. TROTTEBERG (eds), *Multigrid Methods*, Lecture Notes in Mathematics 960, Springer-Verlag, Berlin, Heidelberg, New York, 1982.
- [10] HEMKER, P.W., *On the comparison of line-Gauss-Seidel and ILU relaxation in multigrid algorithms*, In: J.J.H. Miller (ed.), *Computational and asymptotic methods for boundary and interior layers*, pp. 269-277. Boole Press, Dublin, 1982.
- [11] HEMKER, P.W., *Numerical aspects of singular perturbation problems*, In: *Asymptotic Analysis II* (F. Verhuist ed.) Springer LNM 985, pp. 267-287, 1983.
- [12] HEMKER, P.W., R. KETTLER, P. WESSELING & P.M. de ZEEUW, *Multigrid methods: development of fast solvers*, To appear in: *Applied Mathematics and Computation*.
- [13] HEMKER, P.W. & J.J.H. MILLER (eds), *Numerical Analysis of Singular Perturbation problems*, Academic Press, London, 1979.

- [14] JOHNSON, C. & U. NÄVERT, *Analysis of some finite element methods for advection-diffusion problems*, In [3], pp. 99-116.
- [15] KETTLER, R., *Analysis and comparison of relaxation schemes in robust multigrid and preconditioned conjugate gradient methods*, In [9], pp. 502-534.
- [16] KETTLER, R. & J.A. MEIJERINK, *A multigrid method and a combined multigrid conjugate gradient method for elliptic problems with strongly discontinuous coefficients in general domains*, KSEPL Publication 604, Kon. Shell Expl. and Prod. Lab., Rijswijk, The Netherlands, 1981.
- [17] MEIJERINK, J.A. & H.A. van der VORST, *An iterative solution method for linear systems of which the coefficient matrix is a symmetric M-matrix*. Math. Comp. 31, 148-162, 1977.
- [18] MILLER, J.J.H. (ed.), *Boundary and Interior Layers—Computational and Asymptotic Methods*, Boole Press, Dublin, 1980.
- [19] STÜBEN, K. & U. TROTTEBERG, *Multigrid Methods: Fundamental Algorithms, Model Problem Analysis and Applications*. In [9], pp. 1-176.
- [20] WESSELING, P., *Theoretical and practical aspects of a multigrid method*. SIAM J.S.S.C. 3 (1982) 387-407.
- [21] WESSELING, P., *A robust and efficient multigrid method*. In [9], pp. 614-630.
- [22] DE ZEEUW, P.M. & E.J. van ASSELT, *The convergence rate of multi-level algorithms applied to the convection-diffusion equations*. Report NW 142/82, Mathematical Center, Amsterdam, 1982.